Plant Physiology and Biochemistry 232 (2026) 111151

Contents lists available at ScienceDirect

Plant Physiology and Biochemistry

journal homepage: www.elsevier.com/locate/plaphy

Buckwheat FeAUR3 enhances drought tolerance via a melatonin feedback loop

Zhanyu Wang [a,1], Luping Ma [b,1], Chunyun Zhou [a,1], Mengyu Zhao [c], Jia Yang [a], Yongzhi Qi [d], Zemiao Tian [a], Lixia Cao [e], Muriel Quinet [f], Yu Meng [a,*], Jiadong He [g,**]

[a] College of Landscape Architecture and Tourism, Hebei Agricultural University, Baoding, 071001, China
[b] College of Mechanical and Electrical Engineering, Hebei Agricultural University, Baoding, 071000, China
[c] College of Agriculture, Guizhou University, Guiyang, 550025, China
[d] College of Plant Protection, Hebei Agricultural University, Baoding, 071000, China
[e] Zhangjiakou Academy of Agricultural Sciences, Zhangjiakou, 075000, China
[f] Groupe de Recherche en Physiologie végétale, Earth and Life Institute, Université catholique de Louvain-UCLouvain, Louvain-la-Neuve, 1348, Belgium
[g] New Cornerstone Science Laboratory, Key Laboratory of Plant Carbon Capture, CAS Center for Excellence in Molecular Plant Sciences, Institute of Plant Physiology and Ecology, Chinese Academy of Sciences, Shanghai, 200032, China

ARTICLE INFO

Handling Editor: Shivendra Sahi

Keywords:
Abiotic stress
Fagopyrum esculentum
Aurora kinase
Antioxidant system
Osmotic adjustment
Transcriptional regulation

ABSTRACT

Aurora kinases are pivotal regulators of cell division, yet their roles in plant abiotic stress responses remain largely unexplored. While melatonin is a well-established protectant against drought, the upstream genetic pathways governing its biosynthesis under stress are not fully understood, limiting our ability to engineer robust drought tolerance. Here, we identify the buckwheat Aurora kinase, FeAUR3, as a critical upstream regulator of the melatonin-mediated drought response. In transgenic *Arabidopsis*, overexpression lines exhibited a marked enhancement in antioxidant capacity, with superoxide dismutase (SOD) and peroxidase (POD) activities increasing by up to 3.75-fold and 3.35-fold, respectively, alongside a 66.14% increase in proline accumulation and a 37.50% reduction in H_2O_2 content. Similarly, in buckwheat hairy roots, *FeAUR3* overexpression strongly activated the antioxidant system, elevating SOD activity by up to 7.50-fold. Mechanistically, the nucleus-localized FeAUR3 directly upregulates the expression of melatonin biosynthesis genes *FeAANAT* and *FeHIOMT*, leading to a 23.6% elevation in endogenous melatonin levels, which initiates a coordinated defense response. Furthermore, we discovered that melatonin acts as an upstream positive regulator, further inducing *FeAUR3* expression (by 1.12-fold under drought) to form a positive feedback loop that amplifies stress signaling. Molecular docking and dynamics simulations confirmed that melatonin stably binds to FeAUR3 with high affinity (binding energy: −7.2 kcal mol^{-1}). In summary, this study elucidates a FeAUR3-melatonin regulatory module that orchestrates drought adaptation in plants via a synergistic positive feedback loop and a dual defense mechanism. Our findings extend the functional paradigm of Aurora kinases into abiotic stress biology and establish FeAUR3 as a mechanistically validated target for engineering drought-resilient crops.

1. Introduction

Drought stress (DS) stands as one of the most severe abiotic constraints limiting global agricultural productivity and threatening food security (Seleiman et al., 2021). For instance, data from the Food and Agriculture Organization of the United Nations indicates that drought leads to an annual reduction of 10-15% in global crop yields (Galan et al., 2024). Projections indicate that escalating climate change will intensify the frequency and severity of drought events, posing a formidable challenge to sustainable agriculture and ecosystem stability (Gebrechorkos et al., 2025). By inducing cellular water deficit, triggering oxidative damage through the overproduction of reactive oxygen

This article is part of a special issue entitled: Plant Signalling Molecules published in Plant Physiology and Biochemistry.

* Corresponding author.
** Corresponding author.
E-mail addresses: my131sohu@126.com (Y. Meng), hejiadong@cemps.ac.cn (J. He).

[1] These authors have contributed equally to this work as co-first authors.

https://doi.org/10.1016/j.plaphy.2026.111151
Received 3 November 2025; Received in revised form 19 January 2026; Accepted 16 February 2026
Available online 17 February 2026

species (ROS), and impairing photosynthetic efficiency, DS culminates in substantial reductions in crop yield and quality (Kumari et al., 2022). Consequently, elucidating the intricate molecular networks that govern plant responses to drought is of paramount importance for developing climate-resilient crops.

To survive under water-limiting conditions, plants have evolved sophisticated defense mechanisms, primarily centered on the activation of antioxidant and osmotic adjustment systems (He et al., 2020). The antioxidant system, which includes enzymatic antioxidants such as superoxide dismutase (SOD), peroxidase (POD), and catalase (CAT), and non-enzymatic antioxidants such as glutathione and ascorbate, works synergistically to scavenge and regulate ROS levels, thereby protecting cellular components from oxidative damage. Concurrently, the osmotic adjustment system maintains cellular turgor and water balance through the accumulation of compatible solutes, including proline (Pro) and soluble sugar (Ss) (Li et al., 2024b). While the roles of these individual pathways are well-studied, the higher-order regulatory mechanisms that coordinate their synergistic action remain to be fully uncovered. The use of plant growth regulators, including melatonin, has emerged as a promising strategy to enhance drought tolerance by modulating these systems (Raza et al., 2024).

Melatonin (MT), a pleiotropic signaling molecule, has emerged as a master regulator of plant stress tolerance. Synthesized from tryptophan, with aralkylamine N-acetyltransferase (AANAT) and N-acetylserotonin O-methyltransferase (HIOMT) as key rate-limiting enzymes, MT enhances drought resilience by modulating a wide array of physiological processes (Meng et al., 2024). It fortifies the antioxidant machinery, improves ion homeostasis, and upregulates stress-responsive transcription factors and genes, thus orchestrating a comprehensive defense response (Zhao et al., 2021; Khan et al., 2024; Li et al., 2024a). For instance, in tomato seedlings, MT mitigates drought stress by modulating osmotic adjustment through increased sucrose synthesis and fine-tuning ABA signaling (Jahan et al., 2024).

The Aurora kinases, a conserved family of serine/threonine kinases, are canonical regulators of cell division in eukaryotes. In plants, they are integral to chromosome segregation and cytokinesis (Deng et al., 2024). Beyond this classical role, a growing body of evidence suggests that Aurora kinases serve as critical nodes integrating developmental signals and environmental stress. Studies indicate that plant Aurora kinases participate in regulating DNA damage response, oxidative stress homeostasis, and microtubule cytoskeleton reorganization through phosphorylation of specific substrates, processes that are crucial for plant adaptation to abiotic stress. For example, AUR3 has been identified as a critical positive regulator of salt tolerance in *Arabidopsis*, suggesting a functional nexus between cell cycle machinery and stress signaling pathways (Lu et al., 2025). Furthermore, research has demonstrated that its homolog AUR1 is directly involved in the plant response to UV-B radiation stress. It was found that UV-B stress induces AUR1 expression, and overexpression of AUR1 can significantly enhance plant tolerance to UV-B, alleviating damage such as aberrant chromosome segregation (Wang et al., 2021a). These findings collectively indicate that members of the Aurora kinase family play conserved and key roles in plant responses to multiple abiotic stresses. Meanwhile, melatonin, as an important stress-resistant hormone, has been fully demonstrated to enhance the tolerance of plants to various stresses such as drought and waterlogging (Jahan et al., 2025). However, whether these two critical pathways intersect, particularly whether melatonin executes its function by modulating Aurora kinases, remains an unresolved question.Plant drought tolerance is an integrative trait that relies not on isolated pathways, but on the synergistic coordination of downstream effector systems, most critically, the ROS-scavenging antioxidant system and the water-balancing osmotic adjustment system (Zhu, 2016). Drought presents the ideal context to dissect this synergy because it concurrently and directly induces both oxidative stress and osmotic imbalance, thereby engaging both effector systems in a coupled manner.

Although the significance of MT and Aurora has been widely recognized, with MT being a well-known substance that can enhance antioxidant capacity and promote osmotic adjustment, and Aurora kinase having demonstrated potential beyond cell division as a stress response regulator, the direct functional connection between the two, especially in the context of drought, remains unclear (Weimer et al., 2016). Research has yet to explore whether MT's protective effects are mediated through cell cycle-related kinases or if these pathways operate independently. A pivotal unanswered question is whether a MT-Aurora kinase signaling axis exists and if it can synergistically orchestrate the antioxidant and osmotic adjustment systems to confer robust drought tolerance.

Buckwheat (*Fagopyrum esculentum*), an economically important pseudo-cereal, is renowned for its inherent resilience to drought, making it an excellent model for dissecting novel stress tolerance mechanisms (Pinski et al., 2025). While previous work has identified numerous drought-responsive genes in buckwheat, the specific functions of its Aurora kinases in this context are unknown (Meng et al., 2022).

Based on this knowledge gap, we hypothesized that the buckwheat Aurora kinase FeAUR3 enhances drought tolerance by positively regulating the MT biosynthesis pathway. This, in turn, coordinates the synergistic activation of the antioxidant and osmotic adjustment systems, establishing a “dual-protection” mechanism. To test this hypothesis, we employed a multi-faceted approach combining molecular genetics, physiology, and in silico modeling. This study aimed to: (1) functionally characterize FeAUR3 in DS response; (2) uncover the molecular relationship between FeAUR3 and MT metabolism; and (3) elucidate the synergistic interaction between antioxidant and osmotic systems within this regulatory framework. These findings reveal a previously uncharacterized role of an Aurora kinase in plant drought tolerance, revealing a previously unknown link between cell cycle regulators and MT signaling, and offering new insights and potential targets for engineering climate-resilient crops.

2. Materials and methods

2.1. Plant materials

Experiments were conducted using *Fagopyrum esculentum* (Kangbaotianqiao, KBTQ) and *Arabidopsis thaliana* (Columbia-0 ecotype, Col-0). ‘KBTQ’ buckwheat originates from Kangbao County, Hebei Province, China (located in a temperate continental monsoon climate zone). The seeds were strictly selected to ensure a germination rate of >95%. All experimental materials, equipment, and chemical reagents were provided by the Buckwheat Genetic Resources Innovation Research Team at the Institute of Crop Sciences, Chinese Academy of Sciences. Growth conditions for *Nicotiana benthamiana* used in subcellular localization assays are provided in the Supplementary Methods S1.

2.2. Bioinformatics analysis

2.2.1. Tertiary structure prediction of FeAUR3

The tertiary structure of the FeAUR3 protein was predicted using AlphaFold3 (https://alphafoldserver.com/) based on its amino acid sequence (Table S1). Default parameters were applied, with confidence scores (pLDDT) > 90% used as the threshold for high-reliability regions.

2.2.2. Phylogenetic analysis

Homologous Aurora protein sequences from representative species were retrieved from the NCBI database (Table S3). Multiple sequence alignment was performed using MEGA11 software, and a phylogenetic tree was constructed via the Maximum Likelihood (ML) method with 1000 bootstrap replicates (Tamura et al., 2021). The Jones-Taylor-Thornton (JTT) substitution model was selected.

2.3. Generation of transgenic plants

2.3.1. Arabidopsis overexpression lines

The *FeAUR3* gene was amplified from KBTQ cDNA using 2 × Phanta Max Master Mix (Vazyme, Nanjing, China) with gene-specific primers containing restriction sites (Table S2). The amplified product was cloned into the pCAMBIA1307 vector, and the recombinant plasmid (*FeAUR-1307*) was transformed into *Agrobacterium tumefaciens* GV3101 via the freeze-thaw method. Positive clones were resuspended in a solution containing 5% sucrose and 0.02% Silwet L-77. *Arabidopsis* plants at the flowering stage were transformed using the floral dip method (Clough and Bent, 1998), with excess bacterial solution removed by filter paper. After 24 h of dark incubation, plants were returned to standard conditions until seed maturation. T_0 seeds were sown on 1/2 MS solid medium containing 600 μL L^{-1} hygromycin for selection. Through three consecutive generations of resistance screening and PCR verification, homozygous T_3 generation lines were obtained for subsequent experiments (see Supplementary Methods S3.3, S3.5, S3.7, S3.9 for detailed protocols).

2.3.2. Hairy root overexpression lines

The *FeAUR-1307* plasmid was transformed into *Agrobacterium rhizogenes* Ar1193. Positive and CK strains were resuspended in liquid MS medium. Sterile 15-day-old KBTQ seedlings were cut into 1–2 cm stem segments, and leaf surfaces were gently wounded before immersion in the bacterial suspension for 15 min with agitation (Sarkar et al., 2020). Explants were dried on sterile filter paper, placed on MS medium with double-layered filter paper, and incubated in the dark for 48 h. They were then transferred to MC medium containing 100 μg mL^{-1} cefotaxime and cultured in the dark. After 7–9 days, hairy roots (3–4 cm) were isolated for subculture. Genomic DNA was extracted using the CTAB method (Brandfass and Karlovsky, 2008), and positive transformants were confirmed by PCR and qRT-PCR.

2.4. Experimental treatments

Arabidopsis seeds were sterilized with 75% ethanol for 10 min, followed by absolute ethanol for 10 min, and air-dried aseptically. Seeds were sown on 1/2 MS solid medium, cold-treated at 4 °C for 48 h, and then cultured at 22–27 °C with a 16 h/8 h light/dark photoperiod. After 15 days, uniformly grown seedlings were transplanted into a greenhouse. For the drought stress group, each pot was irrigated once with 50 mL of 20% PEG-6000 solution, after which no additional water was supplied until the end of the experiment; the control group received an equal volume of distilled water. Leaf samples were collected on days 7, 14, 21, and 28 post-treatment for physiological and molecular analyses. SOD and POD activities were measured using nitroblue tetrazolium (NBT) photochemical reduction and guaiacol colorimetric methods, respectively (Wang et al., 2023a). CAT activity was determined following (Huo et al., 2020). Ss and Pro contents were quantified using anthrone and acidic ninhydrin methods, respectively (Bai et al., 2023). Sp content was measured via the Coomassie Brilliant Blue G-250 staining method (Sissolak et al., 2019). H_2O_2 content was determined using a commercial kit (BC3590, Solarbio, Beijing, China). Gene expression levels of *FeAUR3*, *AtHKT1*, *AtGPX1*, *AtCAT*, and *AtAPX* were analyzed via qRT-PCR on day 28 (see Supplementary Methods S2 and S3.1 for details).

Hairy root lines were cultured in 50 mL of 20% PEG-6000 solution in conical flasks with agitation for 28 days to simulate DS. Samples were flash-frozen in liquid nitrogen on days 7, 14, 21, and 28 for physiological measurements (SOD, POD, CAT, Ss, Sp, Pro, H_2O_2) and molecular analyses. Expression levels of *FeAUR3*, *AANAT*, and *HIOMT* were quantified via qRT-PCR, and MT content was measured using an ELISA kit (Shanghai Youxuan Biotech, China) on day 28. Detailed protocols are provided in Supplementary Methods S2 and S3.1.

2.5. Molecular biology analyses

2.5.1. qRT-PCR analysis

Total RNA was extracted using the RNA Easy Plant Tissue Kit (DP452, Tiangen, Beijing, China). cDNA was synthesized using HiScript III RT SuperMix (+gDNA wiper, Vazyme, Nanjing, China). qRT-PCR was performed with Taq Pro Universal SYBR qPCR Master Mix (Vazyme, Nanjing, China) using *FeH3* (*F. esculentum*) and *AtActin* (*A. thaliana*) as reference genes. Primers were designed using NCBI Primer-BLAST (Table S2). Four biological replicates were analyzed. Detailed protocols are provided in Supplementary Methods.

2.5.2. Subcellular localization

The *FeAUR3* open reading frame (ORF) was cloned into the pCAMBIA2300 vector to generate a *FeAUR3*-GFP fusion construct. The recombinant plasmid was transformed into *A. tumefaciens* GV3101 via the freeze-thaw method and transiently expressed in *N. benthamiana* leaves using the agroinfiltration method. Fluorescence was observed using a Zeiss LSM 900 confocal microscope, with an empty GFP vector as the control. Detailed protocols are provided in Supplementary Methods.

2.6. Exogenous MT treatment

KBTQ seedlings were grown in a soil-sand mixture (1:5, v/v) pre-watered 24 h before sowing. Four sterilized seeds were sown per pot and cultured in a greenhouse. At the two-leaf stage, seedlings were transplanted into plastic pots (11 cm diameter, 17 cm height) with 8–10 plants per pot. At the 2–4 leaf stage, plants were divided into groups: the experimental group was sprayed with 200 μM MT (melatonin, ≥99% purity, Sigma, USA) every 2 days at 20:00 for 5 applications until leaves dripped; the control group was sprayed with distilled water. Twelve hours after the final application, DS was induced with 50 mL of 20% PEG-6000 solution (Guo et al., 2022). Pots were rotated 90° daily to ensure uniform light exposure. Leaf samples were collected on days 7, 14, 21, and 28 and stored at −80 °C for physiological measurements. *FeAUR3* expression was quantified via qRT-PCR on day 28 (Supplementary Methods). Treatments included: distilled water (CK); 200 μM MT (MT); distilled water + 20% PEG-6000 (DS); and 200 μM MT + 20% PEG-6000 (MT + DS). Among them, the optimal concentrations of drought stress and exogenous MT treatment were determined through pre-experiments. The specific experimental procedures can be found in Supplementary Information S4.

2.6.1. Biomass measurement

After 28 days, 10 KBTQ seedlings per treatment were harvested. Roots, stems, and leaves were separated, washed, and blotted dry. Fresh weight was measured using a CP214 electronic balance (Ohaus, Shanghai, China). Samples were oven-dried at 105 °C for 30 min, then at 75 °C to constant weight, and dry weight was recorded using an SD101-3 drying oven (Suda, Shanghai, China).

2.6.2. Physiological and biochemical measurements

Maximum photochemical efficiency (Fv/Fm) was measured using a portable chlorophyll (Chl) fluorometer (PRI 200, PSI, Czech Republic) after 30 min of dark adaptation on the 2_{nd}–4_{th} healthy leaves of the main stem, with five replicates per treatment (Huang et al., 2013). Chlorophyll content was determined using 95% ethanol extraction (Scrob et al., 2019). APX activity was measured following (Shi et al., 2024). MDA content was quantified using the thiobarbituric acid (TBA) method (Wang et al., 2023a). Relative electrical conductivity (REC) was measured using a DDS-307 conductivity meter at 25 °C (Lim et al., 2022). The superoxide anion (O_2^-) production rate was measured with an assay kit (BC1290, Solarbio, Beijing, China) as described by Jie et al. (2022). SOD, POD, CAT, Ss, Sp, Pro, and H_2O_2 contents were measured as described above. Detailed protocols are provided in Supplementary Methods S2. The determination of the above indicators was carried out

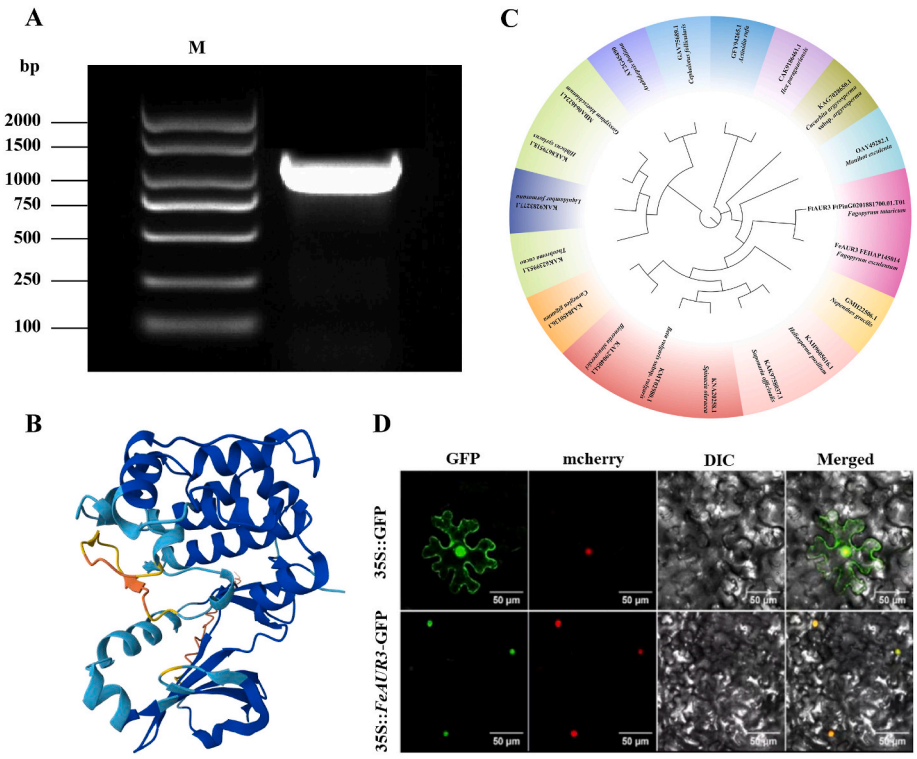

Fig. 1. Molecular characterization and localization of FeAUR3. **(A)** Agarose gel electrophoresis of the amplified *FeAUR3* coding sequence (CDS). **(B)** Predicted three-dimensional structure of FeAUR3 using AlphaFold3. **(C)** Phylogenetic tree of *FeAUR3* and homologous Aurora kinases from other species, constructed via Maximum Likelihood. **(D)** Subcellular localization of FeAUR3-green fluorescent protein (GFP) fusion in *Nicotiana benthamiana* leaves, observed by confocal microscopy.

with four biological replicates.

2.7. Data analysis

All data were initially processed using Microsoft Excel. Statistical analyses were performed with IBM SPSS Statistics 22.0, employing Duncan's multiple range test for mean comparisons at a significance level of $P < 0.05$, with significant differences denoted by lowercase letters (a–d). To systematically evaluate changes in multiple measurement indicators under different treatments, the Max-Min Scaling (MMS) method in SPSSAU (https://spssau.com/) was employed to normalize the data for each indicator to eliminate dimensional differences, and the CNSKnowAll platform (https://cnsknowall.com/) was utilized for integrated multi-index analysis and heatmap visualization. Correlation analysis, PCA, GRA, and partial least squares structural equation modeling (PLS-SEM) were conducted to evaluate relationships among physiological and molecular indices. Graphs were generated using GraphPad Prism 9.0 and Chiplot (https://www.chiplot.online/). GRA was performed using SPSSAU (https://spssau.com/). Path coefficients in PLS-SEM were analyzed using SmartPLS.

2.7.1. Correlation analysis

Pearson correlation analysis was used to assess relationships between physiological and molecular variables, with correlation coefficients ranging from −1 to 1 (Tian et al., 2024). The Pearson correlation coefficient (R) was calculated using the following formula:

$$R = \sum (X_i - X_{av}) \times (Y_i - Y_{av}) \div \sqrt{\sum (X_i - X_{av})^2 \times \sum (Y_i - Y_{av})^2}$$

where (X_i) and (Y_i) represent the measured values of two variables, and X_{av} and Y_{av} denote their respective means.

2.7.2. PLS-SEM construction

To elucidate interactions among 11 physiological indices (encompassing antioxidant enzyme activities, membrane stability, and osmotic adjustment parameters), PLS-SEM was applied (Wang et al., 2023b). Data were preprocessed to address missing values, outliers, and standardization. A theoretical model was constructed using the path weighting scheme, defining relationships between latent and observed variables. Model reliability and validity were evaluated using Composite Reliability (CR), Average Variance Extracted (AVE), and Cronbach's Alpha. Path coefficients and correlations were assessed to validate the structural model.

2.7.3. Molecular docking

MT (PubChem CID: 896) was docked with five target proteins (*FeSOD*, *FePOD*, *FeCAT*, *FeSOS1*, and *FeAVP1*) following established protocols (Lai et al., 2024). The 3D structure of MT was retrieved from PubChem, converted to PDB format using PyMOL 3.0 (Kim et al., 2025), and optimized with AutoDockTools-1.5.7. Homology models of target proteins were generated using SWISS-MODEL, processed for water removal and energy minimization, and docked using AutoDock Vina. Binding affinities (kcal·mol^{-1}) were quantified, and the highest-affinity complexes were visualized with PyMOL.

2.7.4. Molecular dynamics simulation

Molecular dynamics simulations (100 ns) were performed using GROMACS 2020.6 on the highest-affinity MT–protein complexes (Yuk et al., 2022). Proteins were parameterized with the CHARMM36 force field, and ligand topologies were generated using CGenFF. Systems were solvated in a cubic TIP3P water box, neutralized with Na^+/Cl^- ions, and optimized via energy minimization and equilibration (NVT and NPT ensembles). Trajectories were analyzed for RMSD, root-mean-square fluctuation (RMSF), radius of gyration (Rg), solvent-accessible surface area (SASA), and hydrogen bond dynamics.

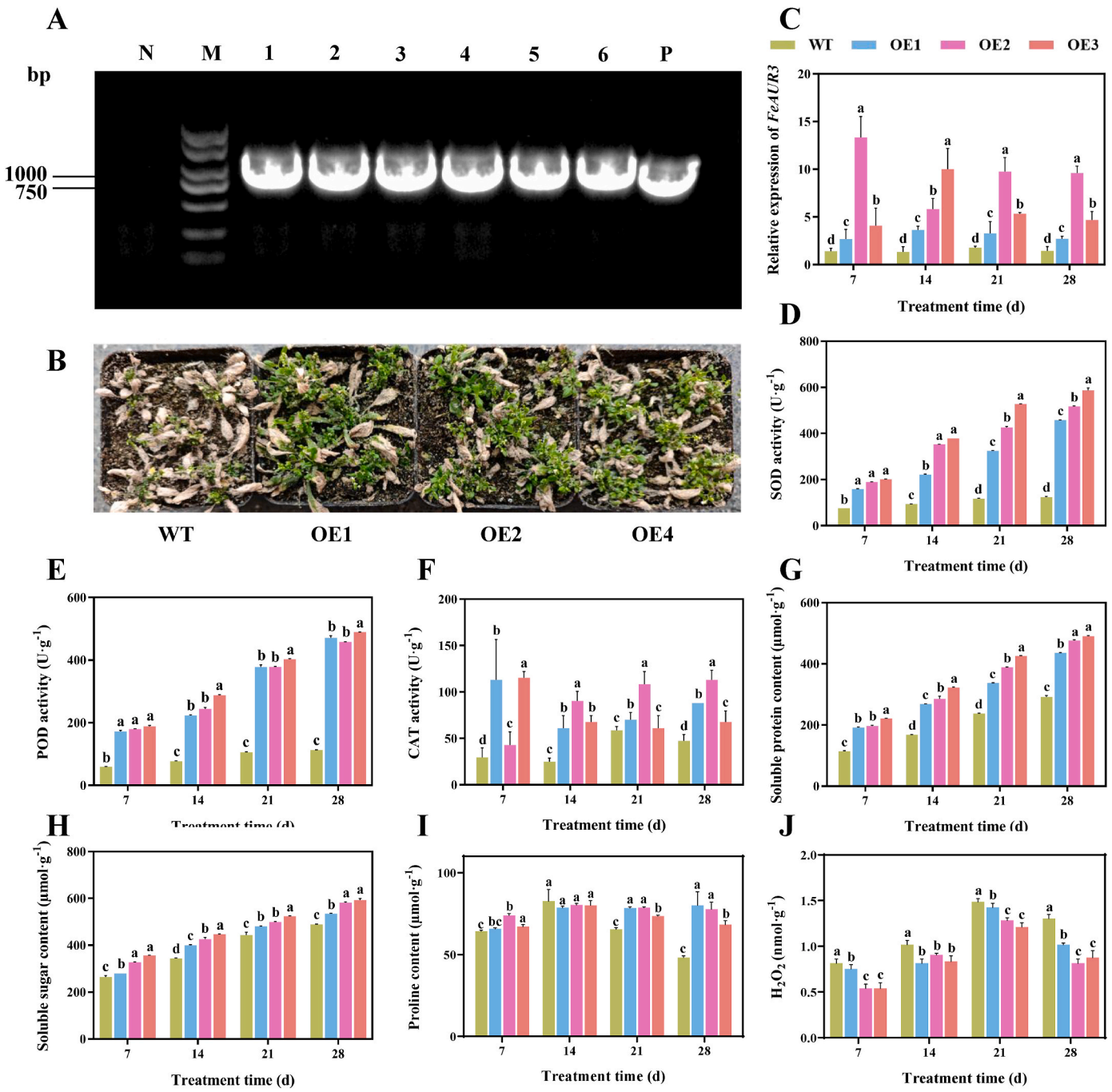

Fig. 2. Drought tolerance analysis of *FeAUR3*-overexpressing Arabidopsis. **(A)** Molecular identification of transgenic Arabidopsis lines. M: DL2000 Plus DNA marker; Lane P: positive control; Lane N: negative control; lanes 1-6: transgenic lines. **(B)** Phenotypic images of Arabidopsis under drought stress. **(C)** Relative expression of *FeAUR3*. **(D)** Superoxide dismutase (SOD) activity. **(E)** Peroxidase (POD) activity. **(F)** Catalase (CAT) activity. **(G)** Soluble protein (Sp) content. **(H)** Soluble sugar (Ss) content. **(I)** Proline (Pro) content. **(J)** Hydrogen peroxide (H_2O_2) content. Data are means ± SD (n = 3), with different letters indicating significant differences ($P < 0.05$) compared to wild-type (WT) at each time point. WT: wild-type Arabidopsis; OE1, OE2, OE3: *FeAUR3*-overexpressing transgenic lines.

3. Results

3.1. Screening, molecular characterization and subcellular localization of *FeAUR3*

The identification of *FeAUR3* was grounded in our prior genomic research on Tartary buckwheat (*Fagopyrum tataricum*). Previously, through a genome-wide association study (GWAS) of 193 germplasm resources, we identified *FtAUR3* as a significant candidate gene associated with abiotic stress tolerance (Lu et al., 2025). Given the close evolutionary proximity between common buckwheat (*Fagopyrum esculentum*) and Tartary buckwheat, we performed a phylogenetic analysis to identify the ortholog of *FtAUR3* in *F. esculentum*, designated as *FeAUR3* (Fig. 1A).

The coding sequence (CDS) of *FeAUR3* was cloned from *Fagopyrum esculentum*. Agarose gel electrophoresis confirmed the amplification of a 906 bp fragment, consistent with the expected CDS length (Fig. 1A). Bioinformatics analysis indicated that *FeAUR3* encodes a protein of 300 amino acids with a molecular weight of 35.3 kDa and a theoretical isoelectric point (pI) of 9.34. The molecular formula was determined as

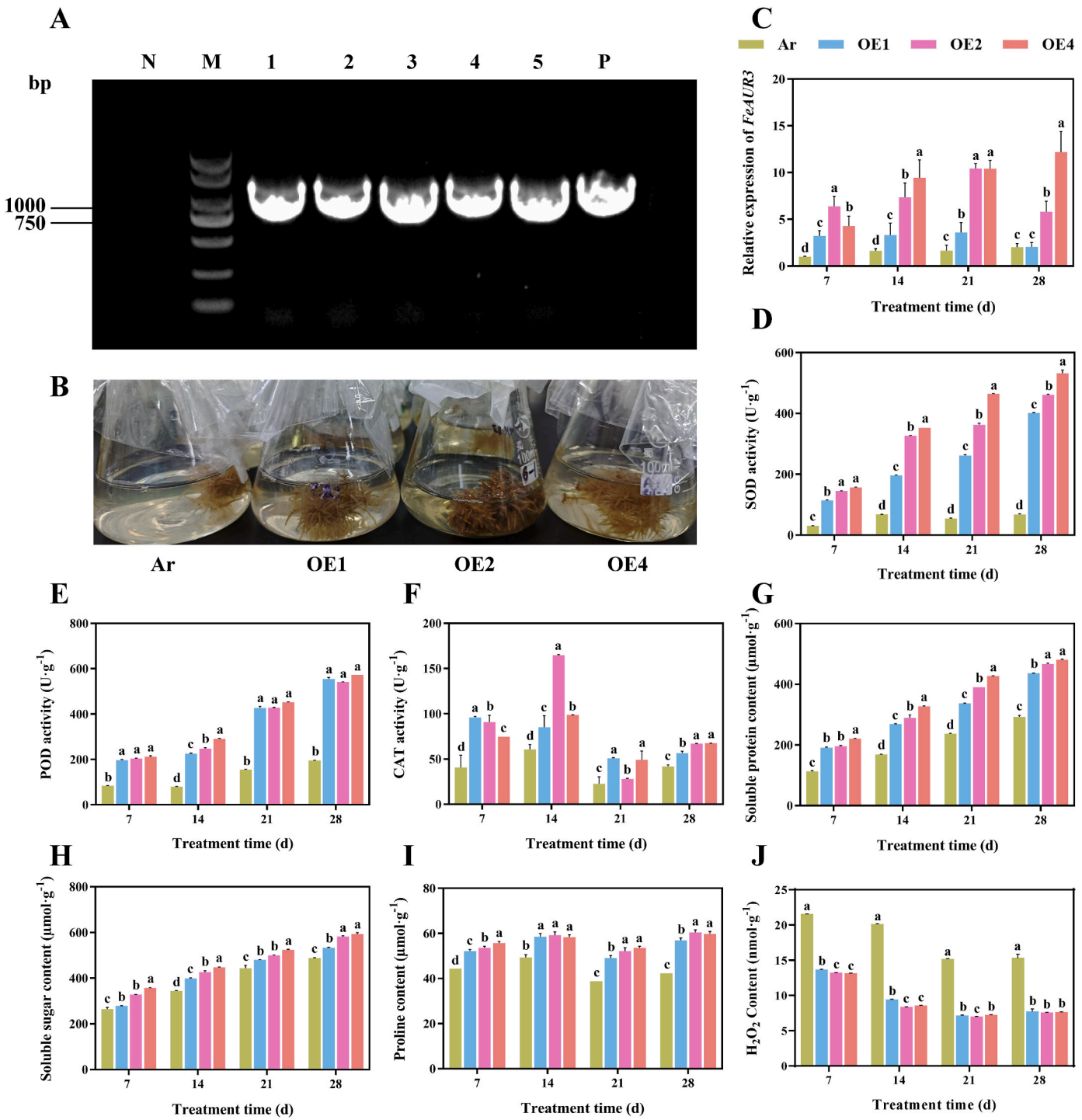

Fig. 3. Drought tolerance analysis of *FeAUR3*-overexpressing buckwheat hairy roots. **(A)** Molecular identification of transgenic buckwheat hairy root lines. M: DL2000 Plus DNA marker; Lane P: positive control; Lane N: negative control; lanes 1-5: transgenic lines. **(B)** Phenotypic images of hairy roots under drought stress. **(C)** Relative expression of *FeAUR3*. **(D)** SOD activity. **(E)** POD activity. **(F)** CAT activity. **(G)** Sp content. **(H)** Ss content. **(I)** Pro content. **(J)** H_2O_2 content. Data are means ± SD (n = 3), with different letters indicating significant differences ($P < 0.05$) compared to the empty vector control (Ar) at each time point. Ar: control; OE1, OE2, OE4: *FeAUR3*-overexpressing hairy root lines.

$C_{1593}H_{2496}N_{452}O_{442}S_8$. The amino acid composition included high proportions of Leucine (11.0%), Lysine (9.0%), Glutamic acid (6.7%), and Glutamine (6.3%). The instability index was 40.7, indicating relative instability, while the aliphatic index was 85.8 and the grand average of hydropathicity (GRAVY) was 0.666, suggesting a hydrophobic nature (Table S1).

The three-dimensional structure of the FeAUR3 protein was predicted using AlphaFold3, revealing a compact α/β globular fold with multiple α-helices and β-sheets forming two interconnected domains, providing a structural basis for its functional domains and substrate binding (Fig. 1B). A phylogenetic tree, constructed using the Maximum Likelihood method with homologous Aurora proteins from representative species, showed *FeAUR3* clustering closely with *FtAUR3*, indicating a close evolutionary relationship (Fig. 1C).

Subcellular localization of FeAUR3 was determined by transient expression of a FeAUR3-GFP fusion protein in *Nicotiana benthamiana*

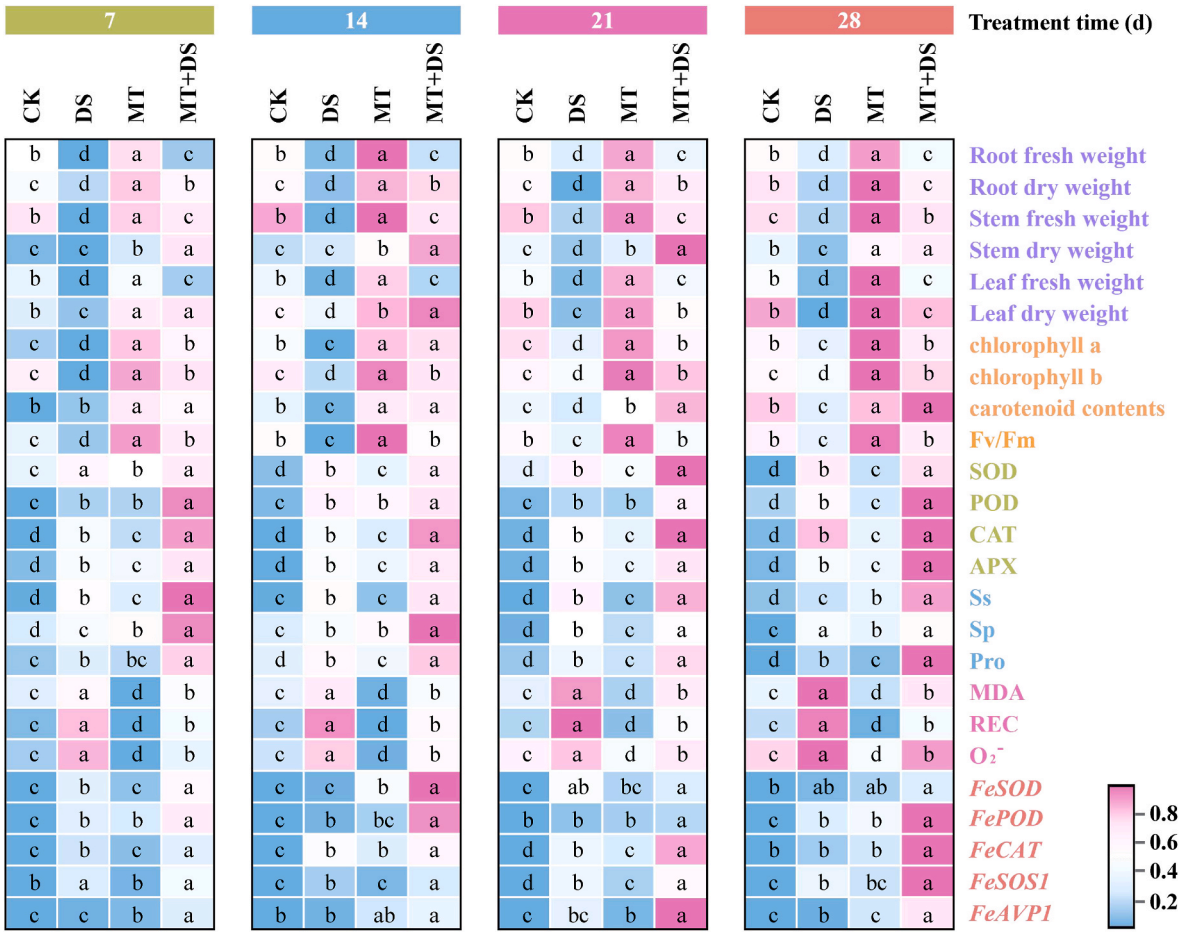

Fig. 4. Integrated heatmap of physiological, biochemical, and molecular responses of buckwheat seedlings to drought stress and exogenous melatonin treatment. Malondialdehyde (MDA), relative electrical conductivity (REC), superoxide anion (O_2^-), superoxide dismutase (SOD), peroxidase (POD), catalase (CAT), ascorbate peroxidase (APX), soluble sugar (Ss), soluble protein (Sp), proline (Pro), chlorophyll *a* (Ca), chlorophyll *b* (Cb), carotenoid (Cc), maximum photochemical efficiency of photosystem II (Fv/Fm). Data are means ± SD (n = 3). For each sampling day, different letters above the bars indicate significant differences among treatments ($P < 0.05$) as determined by one-way ANOVA followed by a post-hoc test. Treatments: CK (distilled water), DS (distilled water + 20% PEG-6000), MT (200 μM melatonin), MT + DS (200 μM melatonin +20% PEG-6000).

leaves. Confocal laser scanning microscopy revealed that the GFP signal was predominantly localized in the nucleus, whereas the control GFP signal was distributed throughout the cell, suggesting that FeAUR3 functions within the nucleus (Fig. 1D).

3.2. Overexpression of *FeAUR3* confers drought tolerance

3.2.1. Functional validation in transgenic arabidopsis

Transgenic T1 generation Arabidopsis plants were obtained via *Agrobacterium tumefaciens* (GV3101)-mediated transformation. Genomic DNA was extracted from leaf tissue and subjected to PCR analysis to confirm the integration of the transgene. As shown in Fig. 2A, the expected target band was detected in lines 1–6, indicating they were positive transgenic plants, while no band was observed in the negative control (empty vector pCAMBIA1307).

Three homozygous T3 overexpression lines (*FeAUR3*-OE1, -OE2, and -OE3), along with wild-type (WT), were selected for drought tolerance phenotyping. Following drought treatment, all lines exhibited mild wilting at 14 days, with the empty vector controls showing slightly more severe symptoms compared to the transgenic lines. By 28 days of treatment, wilting became pronounced in the empty vector controls, whereas the transgenic lines maintained a relatively better physiological state (Fig. 2B).

3.2.1.1. FeAUR3 expression and phenotypic response under DS. Under drought conditions, *FeAUR3* expression was significantly higher in all transgenic lines compared to WT at all time points (Fig. 2C). In the OE2 line, *FeAUR3* expression increased by 8.51-, 3.37-, 4.51-, and 5.64-fold on days 7, 14, 21, and 28, respectively. The OE1 and OE3 lines also exhibited significant increases in *FeAUR3* expression throughout the stress period.

3.2.1.2. Physiological and biochemical responses. DS significantly increased the activities of SOD, POD, and CAT in the transgenic lines compared to WT (Fig. 2D–F). SOD activity in OE1, OE2, and OE3 was 2.70-, 3.18-, and 3.75-fold higher than in WT on day 28, respectively (Fig. 2D). POD activity was 3.19-, 3.07-, and 3.35-fold higher (Fig. 2E). CAT activity was elevated in the transgenic lines, with the largest increases observed in OE3 on day 7 (2.92-fold) and OE2 on day 14 (2.64-fold) compared to WT (Fig. 2F).

Overexpression of *FeAUR3* increased the accumulation of osmolytes (Sp, Ss, and Pro) under DS (Fig. 2G–I). Soluble Protein (Sp) and Ss contents were significantly higher in all OE lines than in WT at all time points. The OE3 line showed the highest Sp content, with increases of 93.84% and 92.03% on days 7 and 14, respectively (Fig. 2G and H). Pro content was significantly higher in the transgenic lines, particularly on day 28, with levels in OE1, OE2, and OE3 being 66.14%, 61.24%, and 41.65% higher than in WT, respectively (Fig. 2I).

The transgenic lines exhibited significantly lower Hydrogen peroxide (H_2O_2) content compared to WT throughout the drought treatment

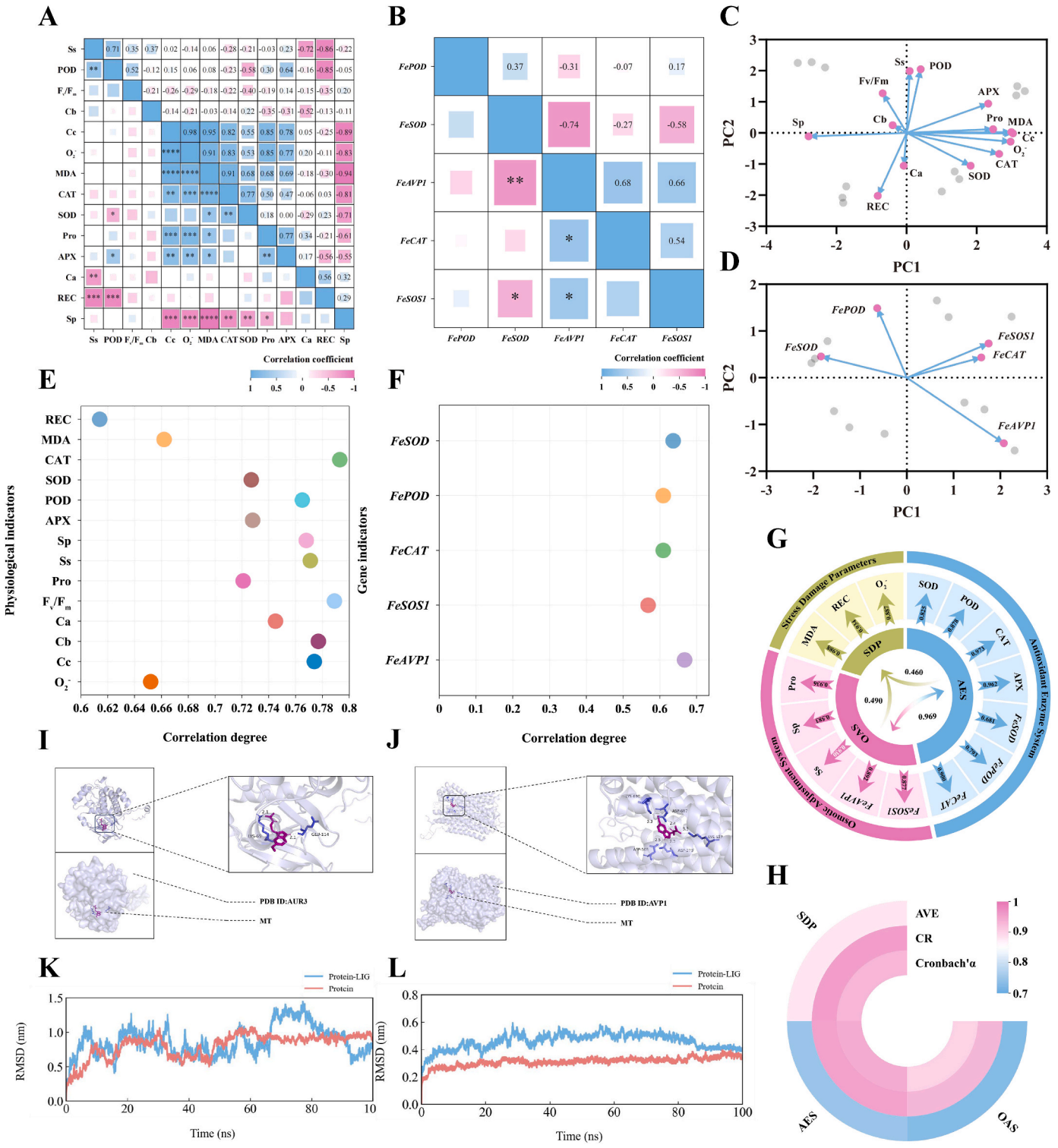

Fig. 5. Comprehensive analysis of drought resistance in buckwheat seedlings. **(A)** Correlation analysis of physiological indicators. **(B)** Correlation analysis of gene expression patterns. **(C)** Principal component analysis (PCA) of physiological indicators. **(D)** PCA of gene expression patterns. **(E)** Grey relational analysis of physiological indicators. **(F)** Grey relational analysis of gene expression patterns. **(G)** Partial least squares structural equation modeling (PLS-SEM) showing relationships among antioxidant enzyme system (AES), osmotic adjustment system (OAS), and stress damage parameters (SDP). Single-headed arrows indicate path coefficients (absolute values); double-headed arrows indicate correlation coefficients; arrows to observed variables show loading coefficients. **(H)** Reliability and validity test results for the PLS-SEM model. **(I)** Molecular docking of melatonin (MT) with FeAUR3, showing interaction sites and binding conformation. **(J)** Molecular docking of MT with FeAVP1, showing interaction sites and binding conformation. **(K)** Root-mean-square deviation (RMSD) of the FeAUR3-MT complex during a 100-ns molecular dynamics simulation. **(L)** RMSD of the FeAVP1-MT complex during a 100-ns molecular dynamics simulation.

(Fig. 2J). On day 28, H_2O_2 levels were reduced by 21.87%, 37.50%, and 32.81% in OE1, OE2, and OE3, respectively, relative to WT.

3.2.1.3. Expression of stress-responsive genes. Expression levels of the ion transporter gene *AtHKT1* and antioxidant enzyme genes *AtGPX1*, *AtCAT*, and *AtAPX* were significantly upregulated in the *FeAUR3*-overexpressing lines compared to WT under DS (Fig. S1A–D). The OE2 and OE3 lines showed the most pronounced upregulation. For example, *AtHKT1* expression in OE2 was 19.27-fold higher than in WT on day 21 (Fig. S1A). On day 28, *AtCAT* and *AtAPX* expression in OE3 were 11.34- and 10.12-fold higher than in WT, respectively (Fig. S1C–D).

3.2.2. Functional validation in transgenic buckwheat hairy roots

Hairy roots were successfully induced via Agrobacterium rhizogenes strain Ar1193-mediated transformation. Genomic DNA was extracted from the roots and subjected to PCR analysis. As shown in Fig. 3A, root lines 1 to 5 were confirmed to be transgenic positive, while no target band was amplified in the negative control (empty vector 1307).

Subsequently, empty vector-transformed control roots (Ar) and three transgenic positive lines with comparable growth vigor (*FeAUR3*-OE1, -OE2, and -OE4) were selected and transferred to liquid medium containing 20% PEG-6000 for simulated drought stress treatment. After 7 days of shake culture, differences in root biomass were observed among the lines. The root biomass of the empty vector control was significantly lower than that of the three transgenic lines (Fig. 3B), suggesting that overexpression of the *FeAUR3* gene may help maintain root growth under osmotic stress.

3.2.2.1. FeAUR3 expression under DS. Under drought treatment, all transgenic hairy root lines exhibited significantly higher *FeAUR3* expression than the Ar control (Fig. 3C). The OE4 line showed the highest expression, with *FeAUR3* levels 3.24-, 4.75-, 5.27-, and 5.00-fold higher than the control on days 7, 14, 21, and 28, respectively.

3.2.2.2. Physiological and biochemical responses. Overexpression of *FeAUR3* in buckwheat hairy roots significantly increased SOD, POD, and CAT activities under DS (Fig. 3D–F). SOD and POD activities were higher in all OE lines compared to the Ar control at all time points. The OE4 line showed the greatest SOD activity increase, reaching 7.50-fold on day 21 (Fig. 3D and E). CAT activity was also higher in the transgenic lines, with varying degrees of enhancement over time (Fig. 3F).

The transgenic hairy root lines accumulated significantly higher levels of Sp, Ss, and Pro compared to the Ar control under drought conditions (Fig. 3G–I). On day 14, Sp content in OE4 was 93.91% higher than in the Ar control (Fig. 3G). On day 28, Pro content in OE2 and OE4 was 42.99% and 41.32% higher, respectively (Fig. 3I).

Overexpression of *FeAUR3* significantly reduced oxidative damage in hairy roots. H_2O_2 content was lower in all OE lines compared to the Ar control throughout the stress period (Fig. 3J). On day 14, H_2O_2 levels were reduced by 53.34%, 58.52%, and 57.48% in OE1, OE2, and OE4, respectively, relative to the control.

3.2.2.3. Expression of MT biosynthesis genes and MT content. Under DS, expression of MT biosynthesis genes *FeAANAT* and *FeHIOMT* was significantly upregulated in all *FeAUR3*-overexpressing hairy root lines compared to the control (Fig. S1F–G). Endogenous MT content was also significantly higher in the OE lines (Fig. S1H). The OE4 line showed a 23.61% increase in MT content on day 14. Correlation analysis indicated that MT content was positively correlated with antioxidant enzyme activities and osmolyte levels, and negatively correlated with oxidative damage indicators (Fig. S1I).

3.3. Exogenous MT alleviates DS in buckwheat seedlings

3.3.1. MT acts as an upstream positive regulator of FeAUR3

Buckwheat seedlings were treated with exogenous MT under control and drought conditions. On day 28, DS alone induced a 1.70-fold increase in *FeAUR3* expression compared to the control (CK). MT treatment alone resulted in a 1.03-fold increase. The combined MT + DS treatment further increased *FeAUR3* expression by 1.12-fold compared to DS alone (Fig. S1J).

3.3.2. Growth and photosynthetic performance

Exogenous MT application increased biomass under DS (Fig. 4). DS reduced fresh and dry weights of roots, stems, and leaves. The MT + DS treatment resulted in significantly higher biomass compared to the DS group at all time points. On day 28, fresh weights of roots, stems, and leaves in the MT + DS group were 0.18-, 0.71-, and 1.11-fold higher, and dry weights were 1.13-, 0.48-, and 0.91-fold higher, respectively, than in the DS group.

Exogenous MT increased photosynthetic parameters under DS (Fig. 4). DS reduced chlorophyll *a*, chlorophyll *b*, carotenoid contents, and maximum photochemical efficiency of PSII (Fv/Fm). The MT + DS treatment resulted in significantly higher levels of all photosynthetic pigments and Fv/Fm compared to the DS group at all time points. On day 14, the Fv/Fm value in the MT + DS group was 85.71% higher than in the DS group.

3.3.3. Physiological and biochemical responses

Exogenous MT increased the activities of SOD, POD, CAT, and APX under DS (Fig. 4). While DS alone induced these enzyme activities, the MT + DS treatment further increased them significantly. On day 7, POD and CAT activities in the MT + DS group were 78.38% and 72.37% higher, respectively, than in the DS group.

Exogenous MT increased the accumulation of osmolytes (Sp, Ss, and Pro) under DS (Fig. 4). Compared to the DS group, the MT + DS treatment resulted in significantly higher Sp, Ss, and Pro levels. On day 28, Ss content was 1.03-fold higher, and Pro content was 29.66% higher in the MT + DS group than in the DS group.

Exogenous MT reduced cellular damage under DS (Fig. 4). DS increased MDA content, O_2^- production rate, and REC. The MT + DS treatment significantly decreased these indicators. On day 28, MDA content was reduced by 16.64% and REC by 39.44% in the MT + DS group compared to the DS group.

3.3.4. Expression of stress-responsive genes

Exogenous MT upregulated the expression of antioxidant genes (*FeSOD*, *FePOD*, *FeCAT*) and osmotic adjustment-related genes (*FeSOS1*, *FeAVP1*) under DS (Fig. 4). Compared to the DS treatment, the MT + DS treatment significantly increased expression of these genes. On day 28, *FeAVP1* expression was 4.64-fold higher in the MT + DS group than in the DS group.

3.4. Integrated analysis of MT-mediated drought tolerance

Correlation analysis, principal component analysis (PCA), grey relational analysis (GRA), and partial least squares-structural equation modeling (PLS-SEM) were performed to evaluate MT-mediated drought tolerance mechanisms.

Correlation analysis showed significant relationships among physiological and molecular indicators (Fig. 5A and B). MDA content was positively correlated with O_2^- ($r = 0.97$, $P < 0.01$) and negatively correlated with Sp content ($r = -0.94$, $P < 0.01$). *FeAVP1* expression was positively correlated with *FeCAT* ($r = 0.68$) and *FeSOS1* ($r = 0.66$).

PCA separated treatment groups (Fig. 5C and D). For physiological indices, PC1 and PC2 explained 44.30% and 25.84% of the total variance, respectively. For gene expression, PC1 and PC2 explained 61.38% and 22.64% of the variance, indicating distinct responses to MT

treatment under DS.

GRA identified key factors influenced by MT (Fig. 5E and F). CAT activity had the highest grey relational grade (0.793) among physiological indices, and *FeAVP1* had the highest grade (0.658) among genes.

PLS-SEM modeled relationships among the antioxidant enzyme system (AES), osmotic adjustment system (OAS), and stress damage parameters (SDP) (Fig. 5G). The model showed high reliability and validity (CR: 0.929–0.956, AVE: 0.729–0.878) (Fig. 5H). Path coefficients indicated that OAS (−0.490) had a stronger negative effect on SDP than AES, with a strong positive correlation between OAS and AES (0.969).

3.5. Molecular docking and dynamics simulation of MT with FeAUR3 and FeAVP1

Molecular docking predicted binding affinities of −7.2 kcal mol^{-1} for FeAUR3-MT and −6.5 kcal mol^{-1} for FeAVP1-MT. MT formed two hydrogen bonds with FeAUR3 residues GLU114 and LYS65, and five hydrogen bonds with FeAVP1 residues LYS690, ASP687, LYS537, ASP279, and ASP503, with additional hydrophobic and electrostatic interactions (Fig. 5I and J).

Molecular dynamics (MD) simulations (100 ns) confirmed the stability of these complexes. For FeAUR3-MT, root-mean-square deviation (RMSD) stabilized after initial fluctuations, with a stable core structure (RMSF), consistent Rg, and SASA values. For FeAVP1-MT, RMSD, Rg, and SASA stabilized after ~60 ns, with key hydrogen bonds maintained, supporting the docking predictions and suggesting that MT modulates FeAUR3 and FeAVP1 function through stable binding (Fig. 5K and L).

4. Discussion

This study elucidates a regulatory pathway in which the buckwheat Aurora kinase, *FeAUR3*, enhances drought tolerance by promoting MT biosynthesis, coordinating antioxidant and osmotic adjustment systems to mitigate DS. These findings expand the known roles of Aurora kinases beyond cell cycle regulation and establish a molecular link between *FeAUR3* and MT-mediated stress responses in plants, particularly in the context of buckwheat's adaptation to arid environments.

Overexpression of *FeAUR3* in Arabidopsis and buckwheat hairy roots increased drought tolerance, as evidenced by elevated activities of antioxidant enzymes (SOD, POD, CAT) and accumulation of osmolytes (Sp, Ss, Pro). This enhancement of the antioxidant system aligns with strategies that bolster innate defense capacities; for instance, exogenous application of the flavonoid antioxidant rutin has been shown to ameliorate salinity-induced oxidative stress and improve germination and early growth in buckwheat (Yang et al., 2025). While Aurora kinases are primarily known for mitotic functions (Eibes et al., 2023), recent studies implicate them in abiotic stress responses, such as aluminum tolerance via organic acid exudation (Van Damme et al., 2011; Komaki et al., 2020; Naso et al., 2021). For instance, they have been linked to aluminum tolerance mechanisms, potentially by facilitating the exudation of organic acids like malate to chelate toxic Al^{3+} ions (Naso et al., 2021). Our results extend this role, showing that *FeAUR3*, localized in the nucleus, upregulates antioxidant enzyme activities and osmolyte synthesis, reducing H_2O_2 and maintaining cellular turgor. The nuclear localization of *FeAUR3* suggests it may phosphorylate transcription factors or chromatin modifiers to regulate stress-responsive genes, a mechanism consistent with Aurora kinases' phosphorylation activity in other systems (Abdul Azeez et al., 2019). This nuclear role likely enables *FeAUR3* to orchestrate downstream responses, though specific TF targets require further investigation.

A key finding of this study is the mechanistic connection between *FeAUR3* and MT, a pleiotropic molecule widely recognized as a master regulator of plant defense against abiotic stresses (Hassan et al., 2022). We demonstrate that *FeAUR3* overexpression upregulates key MT biosynthesis genes (*FeAANAT*, *FeHIOMT*), leading to increased endogenous MT levels in hairy roots (Fig. S1F–G). This suggests that *FeAUR3* enhances drought tolerance, at least in part, by boosting MT production. This finding is strongly supported by extensive research showing that both exogenous MT application and genetic engineering to elevate endogenous MT levels (e.g., overexpression of *MzASMT1* in apple or *TaCOMT* in wheat) significantly improve antioxidant capacity and osmotic adjustment under drought (Zuo et al., 2014; L. Wang et al., 2017; Yang et al., 2019; Altaf et al., 2022). Conversely, disruption of MT biosynthesis in *snat1* mutants or its signaling in *cand2* receptor mutants renders plants more sensitive to DS, underscoring MT's indispensable role (Wang et al., 2021b). Thus, our results place *FeAUR3* as a positive regulator upstream of this critical MT-mediated defense pathway.

Furthermore, our results suggest the existence of a positive feedback loop. Exogenous MT application induced *FeAUR3* expression, an effect that was synergistically amplified under DS (Fig. S1J). This MT treatment also upregulated a cohort of downstream defense genes, including *FeSOD*, *FePOD*, *FeCAT*, *FeSOS1*, and *FeAVP1*. This indicates that MT not only acts downstream of *FeAUR3* but also functions as a signal molecule to amplify the entire defense response. The signaling function of MT is typically mediated by receptors. While the first plant MT receptor, CAND2/PMTR1, has been identified and linked to stomatal regulation (Wei et al., 2018), our molecular docking and dynamics simulations reveal a stable binding interaction between MT and the FeAUR3 protein (−7.2 kcal mol^{-1}), potentially inducing a conformational change to enhance its kinase activity (Fig. S2F–I). This raises the intriguing possibility that FeAUR3 may act as a downstream effector in the MT signaling cascade or even function as a non-canonical MT receptor, complementing the established receptor pathways.

The synergistic regulation of antioxidant and osmotic adjustment systems is a central mechanism of MT-mediated drought tolerance. Our PLS-SEM analysis confirmed a strong positive correlation (0.969) between these two systems, both of which contributed to mitigating stress-induced damage (Fig. 5G). Intriguingly, the osmotic adjustment system exerted a stronger direct protective effect on membrane stability (path coefficient of −0.490) than the antioxidant system. This might reflect a specific adaptation strategy in buckwheat, where rapid osmotic regulation is paramount for survival in arid conditions. This effect is further enhanced by the dual function of osmolytes like Pro, which not only maintains cellular turgor but also acts as a direct radical scavenger (Kebert et al., 2024). Moreover, we observed a fascinating developmental-stage specificity in MT's regulatory targets. GRA analysis identified *FeAVP1*, a vacuolar H^+-pyrophosphatase critical for ion homeostasis and osmotic potential (Hernández et al., 2016), as the most responsive gene to MT in seedlings (0.658 grade), contrasting with the prominence of *FePOD* in seeds. This suggests a strategic shift in defense priorities: from managing oxidative stress during germination (where POD is crucial) to maintaining water and ion homeostasis in vegetative tissues (where AVP1 is vital). The stable MT-FeAVP1 interaction observed in silico (Fig. S2J–M) supports a model of targeted regulation, whereby MT modulates key proteins to fine-tune defense strategies across different developmental stages. Future elucidation of the precise kinetic characteristics of this module, such as its initiation speed, duration, and interaction with other stress signaling networks, would provide key insights into its role in adaptive plasticity under fluctuating stress conditions.

In conclusion, these findings chart a novel regulatory module where the FeAUR3 kinase acts as a key positive regulator of drought tolerance by promoting MT biosynthesis. This initiates a robust defense response involving a synergistic interplay between antioxidant and osmotic systems, which is further amplified by an MT-FeAUR3 feedback loop. Future research should be deepened at two levels. At the mechanistic level, direct phosphorylation targets of FeAUR3 can be identified, and its signaling network can be dissected to confirm its potential receptor-like function. At the translational level, the functional orthology of this module in other crops could be validated, and its potential to stably enhance drought tolerance without compromising yield under agronomically relevant, fluctuating water regimes could be assessed. These

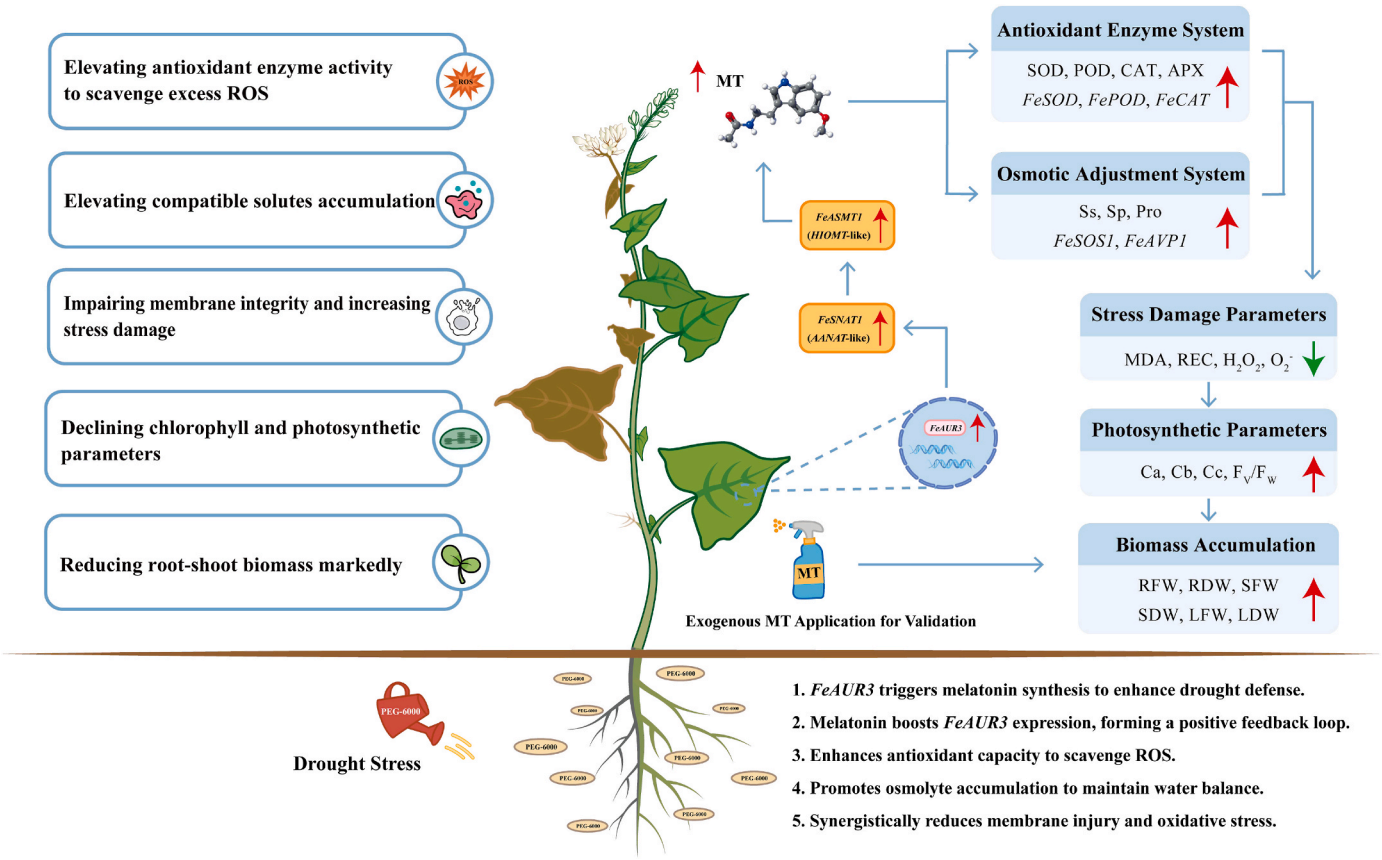

Fig. 6. Mechanism of FeAUR3-melatonin signaling and dual defense in buckwheat drought tolerance. Diagram depicting the mechanism of FeAUR3-melatonin signaling under drought stress. FeAUR3 initiates MT synthesis, forming a positive feedback loop with FeAUR3 expression. The pathway activates antioxidant enzymes (SOD, POD, CAT, APX) and promotes osmolyte accumulation (Ss, Sp, Pro) for dual defense against drought.

investigations will ultimately reveal whether targeting the Aurora kinase-MT hub can serve as a universal strategy for designing climate-resilient crops. Clarifying these mechanisms is of great significance for engineering climate-resilient crops through genetic approaches.

5. Conclusion

This study identifies the buckwheat Aurora kinase, *FeAUR3*, as a novel and pivotal regulator of drought tolerance. We have delineated a sophisticated signaling cascade wherein FeAUR3 initiates MT biosynthesis, which in turn activates a synergistic dual-defense mechanism, coordinating both antioxidant and osmotic adjustment systems. This entire response is further amplified by a positive feedback loop, where MT reinforces *FeAUR3* expression. These findings fundamentally expand the known roles of Aurora kinases beyond cell division into the realm of plant stress biology and establish the *FeAUR3*- MT module as a powerful genetic target for engineering the climate-resilient crops of the future (Fig. 6).

CRediT authorship contribution statement

Zhanyu Wang: Writing – original draft, Visualization, Formal analysis. **Luping Ma:** Writing – original draft, Validation, Methodology. **Chunyun Zhou:** Writing – review & editing, Software, Data curation. **Mengyu Zhao:** Investigation, Writing – review & editing. **Jia Yang:** Writing – review & editing, Formal analysis. **Yongzhi Qi:** Writing – review & editing, Data curation. **Zemiao Tian:** Writing – review & editing, Validation, Investigation. **Lixia Cao:** Writing – review & editing, Resources, Project administration. **Muriel Quinet:** Writing – review & editing, Supervision. **Yu Meng:** Validation, Supervision, Funding acquisition, Conceptualization. **Jiadong He:** Writing – review & editing, Supervision, Conceptualization.

Funding

This work was supported by the Natural Science Foundation of Hebei Province China (C2023204097), the Research Project of Basic Scientifc Research Operating Expenses of Hebei Provincial Universities, China (KY2024055), the National Natural Science Foundation of China (No. 32372045), Yanzhao Golden Platform Talent Gathering Plan Backbone Talent Project of Hebei Province, China (A2025013) and by Zhangjiakou Comprehensive Experiment Station of National Oat and Buckwheat Industry Technology System, China (CARS-07-G-1).

Declaration of competing interest

The authors declare that they have no known competing financial interests or personal relationships that could have appeared to influence the work reported in this paper.

Appendix A. Supplementary data

Supplementary data to this article can be found online at https://doi.org/10.1016/j.plaphy.2026.111151.

Data availability

Data will be made available on request.

References

Abdul Azeez, K.R., Chatterjee, S., Yu, C., Golub, T.R., Sobott, F., Elkins, J.M., 2019. Structural mechanism of synergistic activation of Aurora kinase B/C by phosphorylated INCENP. Nat. Commun. 10, 3166. https://doi.org/10.1038/s41467-019-11085-0.

Altaf, M.A., Shahid, R., Ren, M.-X., Naz, S., Altaf, M.M., Khan, L.U., Tiwari, R.K., Lal, M. K., Shahid, M.A., Kumar, R., Nawaz, M.A., Jahan, M.S., Jan, B.L., Ahmad, P., 2022. Melatonin improves drought stress tolerance of tomato by modulating plant growth, root architecture, photosynthesis, and antioxidant defense system. Antioxidants 11, 309. https://doi.org/10.3390/antiox11020309.

Bai, Y., Zhou, Y., Yue, T., Huang, Y., He, C., Jiang, W., Liu, H., Zeng, H., Wang, J., 2023. Plant growth-promoting rhizobacteria Bacillus velezensis JB0319 promotes lettuce growth under salt stress by modulating plant physiology and changing the rhizosphere bacterial community. Environ. Exp. Bot. 213, 105451. https://doi.org/10.1016/j.envexpbot.2023.105451.

Brandfass, C., Karlovsky, P., 2008. Upscaled CTAB-based DNA extraction and real-time PCR assays for Fusarium culmorum and F. graminearum DNA in plant material with reduced sampling error. Int. J. Math. Stat. 9, 2306–2321. https://doi.org/10.3390/ijms9112306.

Clough, S.J., Bent, A.F., 1998. Floral dip: a simplified method for*Agrobacterium*-mediated transformation of*Arabidopsis thaliana*. Plant J. 16, 735–743. https://doi.org/10.1046/j.1365-313x.1998.00343.x.

Deng, X., Xiao, Y., Tang, X., Liu, B., Lin, H., 2024. Arabidopsis α-Aurora kinase plays a role in cytokinesis through regulating MAP65-3 association with microtubules at phragmoplast midzone. Nat. Commun. 15, 3779. https://doi.org/10.1038/s41467-024-48238-9.

Eibes, S., Rajendraprasad, G., Guasch-Boldu, C., Kubat, M., Steblyanko, Y., Barisic, M., 2023. CENP-E activation by Aurora A and B controls kinetochore fibrous Corona disassembly. Nat. Commun. 14, 5317. https://doi.org/10.1038/s41467-023-41091-2.

Galan, P.-M., Ivanescu, L.-C., Leti, L.-I., Zamfirache, M.M., Gorgan, D.-L., 2024. Comparative effects of water scarcity on the growth and development of two common bean (Phaseolus vulgaris L.) genotypes with different geographic origin (Mesoamerica/Andean). Plants 13, 2111. https://doi.org/10.3390/plants13152111.

Gebrechorkos, S.H., Sheffield, J., Vicente-Serrano, S.M., Funk, C., Miralles, D.G., Peng, J., Dyer, E., Talib, J., Beck, H.E., Singer, M.B., Dadson, S.J., 2025. Warming accelerates global drought severity. Nature 642, 628–635. https://doi.org/10.1038/s41586-025-09047-2.

Guo, Y., Li, D., Liu, L., Sun, H., Zhu, L., Zhang, K., Zhao, H., Zhang, Y., Li, A., Bai, Z., Tian, L., Dong, H., Li, C., 2022. Seed priming with melatonin promotes seed germination and seedling growth of triticale hexaploide L. under PEG-6000 induced drought stress. Front. Plant Sci. 13, 932912. https://doi.org/10.3389/fpls.2022.932912.

Hassan, M.U., Mahmood, A., Awan, M.I., Maqbool, R., Aamer, M., Alhaithloul, H.A.S., Huang, G., Skalicky, M., Brestic, M., Pandey, S., El Sabagh, A., Qari, S.H., 2022. Melatonin-induced protection against plant abiotic stress: mechanisms and prospects. Front. Plant Sci. 13. https://doi.org/10.3389/fpls.2022.902694.

He, J.-D., Zou, Y.-N., Wu, Q.-S., Kuča, K., 2020. Mycorrhizas enhance drought tolerance of trifoliate orange by enhancing activities and gene expression of antioxidant enzymes. Sci. Hortic. 262, 108745. https://doi.org/10.1016/j.scienta.2019.108745.

Hernández, A., Herrera-Palau, R., Madroñal, J.M., Albi, T., López-Lluch, G., Perez-Castiñeira, J.R., Navas, P., Valverde, F., Serrano, A., 2016. Vacuolar H+-Pyrophosphatase AVP1 is involved in amine fungicide tolerance in Arabidopsis thaliana and provides tridemorph resistance in yeast. Front. Plant Sci. 7. https://doi.org/10.3389/fpls.2016.00085.

Huang, J., Zhang, P.-J., Zhang, J., Lu, Y.-B., Huang, F., Li, M.-J., 2013. Chlorophyll content and chlorophyll fluorescence in tomato leaves infested with an invasive Mealybug,*Phenacoccus solenopsis*(Hemiptera: pseudococcidae). Environ. Entomol. 42, 973–979. https://doi.org/10.1603/en12342.

Huo, M., Zhao, L., Wang, T., Zong, W., Liu, R., 2020. Binding mechanism of maltol with catalase investigated by spectroscopy, molecular docking, and enzyme activity assay. J. Mol. Recogn. 33, e2822. https://doi.org/10.1002/jmr.2822.

Jahan, M.S., Hasan, M.M., Siddique, A.B., Zarbakhsh, S., Hamada, M.M., Hussain, M.A., Jabborova, D., Corpas, F.J., 2025. Melatonin's role in enhancing waterlogging tolerance in plants: current understanding and future directions. Physiol. Plantarum 177. https://doi.org/10.1111/ppl.70499.

Jahan, M.S., Yang, J.Y., Althaqafi, M.M., Alharbi, B.M., Wu, H.Y., Zhou, X.B., 2024. Melatonin mitigates drought stress by increasing sucrose synthesis and suppressing abscisic acid biosynthesis in tomato seedlings. Physiol. Plantarum 176, e14457. https://doi.org/10.1111/ppl.14457.

Jie, Z., Liu, J., Shu, M., Ying, Y., Yang, H., 2022. Detection strategies for superoxide anion: a review. Talanta 236, 122892. https://doi.org/10.1016/j.talanta.2021.122892.

Kebert, M., Stojnić, S., Rašeta, M., Kostić, S., Vuksanović, V., Ivanković, M., Lanšćak, M., Markić, A.G., 2024. Variations in proline content, polyamine profiles, and antioxidant capacities among different provenances of European beech (Fagus sylvatica L.). Antioxidants 13, 227. https://doi.org/10.3390/antiox13020227.

Khan, Z., Jan, R., Asif, S., Farooq, M., Jang, Y.-H., Kim, E.-G., Kim, N., Kim, K.-M., 2024. Exogenous melatonin induces salt and drought stress tolerance in rice by promoting plant growth and defense system. Sci. Rep. 14, 1214. https://doi.org/10.1038/s41598-024-51369-0.

Kim, S., Chen, J., Cheng, T., Gindulyte, A., He, J., He, S., Li, Q., Shoemaker, B.A., Thiessen, P.A., Yu, B., Zaslavsky, L., Zhang, J., Bolton, E.E., 2025. PubChem 2025 update. Nucleic Acids Res. 53, D1516–D1525. https://doi.org/10.1093/nar/gkae1059.

Komaki, S., Takeuchi, H., Hamamura, Y., Heese, M., Hashimoto, T., Schnittger, A., 2020. Functional analysis of the plant chromosomal passenger complex. Plant Physiol. 183, 1586–1599. https://doi.org/10.1104/pp.20.00344.

Kumari, V.V., Banerjee, P., Verma, V.C., Sukumaran, S., Chandran, M.A.S., Gopinath, K. A., Venkatesh, G., Yadav, S.K., Singh, V.K., Awasthi, N.K., 2022. Plant nutrition: an effective way to alleviate abiotic stress in agricultural crops. Int. J. Math. Stat. 23, 8519. https://doi.org/10.3390/ijms23158519.

Lai, D., Zhang, K., He, Y., Fan, Y., Li, W., Shi, Y., Gao, Y., Huang, X., He, J., Zhao, H., Lu, X., Xiao, Y., Cheng, J., Ruan, J., Georgiev, M.I., Fernie, A.R., Zhou, M., 2024. Multi-omics identification of a key glycosyl hydrolase gene *FtGH1* involved in rutin hydrolysis in tartary buckwheat (*Fagopyrum tataricum*). Plant Biotechnol. J. 22, 1206–1223. https://doi.org/10.1111/pbi.14259.

Li, J., Li, Y., Du, M., Zang, D., Men, Q., Su, P., Guo, S., 2024a. Exogenous melatonin improves drought stress tolerance via regulating tryptophan metabolism and flavonoid biosynthesis pathways in wheat. Physiol. Plantarum 176, e70006. https://doi.org/10.1111/ppl.70006.

Li, Q., Zhu, P., Yu, X., Xu, J., Liu, G., 2024b. Physiological and molecular mechanisms of rice tolerance to salt and drought stress: advances and future directions. Int. J. Math. Stat. 25, 9404. https://doi.org/10.3390/ijms25179404.

Lim, J.H., Hou, J., Chun, J., Lee, R.D., Yun, J., Jung, J., Lee, C.H., 2022. Importance of hydroxide ion conductivity measurement for alkaline water electrolysis membranes. Membranes 12, 556. https://doi.org/10.3390/membranes12060556.

Lu, X., Zuo, Q., Huda, MdN., Shi, Y., Li, G., Wang, X., Xiao, Y., Khurshid, M., Jahan, T., Dhami, N., Gauchan, D.P., Ali, MdA., Cheng, J., Meng, Y., Ruan, J., Zhou, M., 2025. Genome-wide association analysis locates FtAUR3 in tartary buckwheat that contributes to enhance plant salt resistance. J. Integr. Agric. https://doi.org/10.1016/j.jia.2025.04.008.

Meng, H.-L., Sun, P.-Y., Wang, J.-R., Sun, X.-Q., Zheng, C.-Z., Fan, T., Chen, Q.-F., Li, H.-Y., 2022. Comparative physiological, transcriptomic, and WGCNA analyses reveal the key genes and regulatory pathways associated with drought tolerance in tartary buckwheat. Front. Plant Sci. 13. https://doi.org/10.3389/fpls.2022.985088.

Meng, L., Feng, Y., Zhao, M., Jang, T., Bi, H., Ai, X., 2024. Hydrogen peroxide mediates melatonin-induced chilling tolerance in cucumber seedlings. Plant Cell Rep. 43, 279. https://doi.org/10.1007/s00299-024-03332-6.

Naso, F.D., Boi, D., Ascanelli, C., Pamfil, G., Lindon, C., Paiardini, A., Guarguaglini, G., 2021. Nuclear localisation of Aurora-A: its regulation and significance for Aurora-A functions in cancer. Oncogene 40, 3917–3928. https://doi.org/10.1038/s41388-021-01766-w.

Pinski, A., Mehdi, S.M.M., Betekhtin, A., 2025. Molecular mechanisms underlying abiotic stress responses in buckwheat. Plant Sci. 357, 112526. https://doi.org/10.1016/j.plantsci.2025.112526.

Raza, A., Bhardwaj, S., Rahman, M.A., García-Caparrós, P., Copeland, R.G.R., Charagh, S., Rivero, R.M., Gopalakrishnan, S., Corpas, F.J., Siddique, K.H.M., Hu, Z., 2024. Fighting to thrive via plant growth regulators: green chemical strategies for drought stress tolerance. Physiol. Plantarum 176, e14605. https://doi.org/10.1111/ppl.14605.

Sarkar, J., Misra, A., Banerjee, N., 2020. Genetic transfection, hairy root induction and solasodine accumulation in elicited hairy root clone of Solanum erianthum D. Don. J. Biotechnol. 323, 238–245. https://doi.org/10.1016/j.jbiotec.2020.09.002.

Scrob, T., Hosu, A., Cimpoiu, C., 2019. The influence of in vitro gastrointestinal digestion of Brassica oleracea florets on the antioxidant activity and chlorophyll, carotenoid and phenolic content. Antioxidants 8, 212. https://doi.org/10.3390/antiox8070212.

Seleiman, M.F., Al-Suhaibani, N., Ali, N., Akmal, M., Alotaibi, M., Refay, Y., Dindaroglu, T., Abdul-Wajid, H.H., Battaglia, M.L., 2021. Drought stress impacts on plants and different approaches to alleviate its adverse effects. Plants 10, 259. https://doi.org/10.3390/plants10020259.

Shi, J., Wang, Y., Fan, X., Li, R., Yu, C., Peng, Z., Gao, Y., Liu, Z., Duan, L., 2024. A novel plant growth regulator B2 mediates drought resistance by regulating reactive oxygen species, phytohormone signaling, phenylpropanoid biosynthesis, and starch metabolism pathways in Carex breviculmis. Plant Physiol. Biochem. 213, 108860. https://doi.org/10.1016/j.plaphy.2024.108860.

Sissolak, B., Zabik, C., Saric, N., Sommeregger, W., Vorauer-Uhl, K., Striedner, G., 2019. Application of the Bradford assay for cell lysis quantification: residual protein content in cell culture supernatants. Biotechnol. J. 14, 1800714. https://doi.org/10.1002/biot.201800714.

Tamura, K., Stecher, G., Kumar, S., 2021. MEGA11: molecular evolutionary genetics analysis version 11. https://pubmed.ncbi.nlm.nih.gov/33892491/.

Tian, Z., Zhao, M., Wang, J., Yang, Q., Ma, Y., Yang, X., Ma, L., Qi, Y., Li, J., Quinet, M., Shi, B., Meng, Y., 2024. Exogenous melatonin improves germination rate in buckwheat under high temperature stress by regulating seed physiological and biochemical characteristics. PeerJ 12, e17136. https://doi.org/10.7717/peerj.17136.

Van Damme, D., De Rybel, B., Gudesblat, G., Demidov, D., Grunewald, W., De Smet, I., Houben, A., Beeckman, T., Russinova, E., 2011. *Arabidopsis*α Aurora kinases function in formative cell division plane orientation. Plant Cell 23, 4013–4024. https://doi.org/10.1105/tpc.111.089565.

Wang, J., Yan, X., Chen, H., Feng, J., Han, R., 2021a. Enhanced UV-B radiation affects AUR1 regulation of mitotic spindle morphology leading to aberrant mitosis. Plant Physiol. Biochem. 159, 160–170. https://doi.org/10.1016/j.plaphy.2020.12.017.

Wang, L., Feng, C., Zheng, X., Guo, Y., Zhou, F., Shan, D., Liu, X., Kong, J., 2017. Plant mitochondria synthesize melatonin and enhance the tolerance of plants to drought stress. J. Pineal Res. 63, e12429. https://doi.org/10.1111/jpi.12429.

Wang, L.-F., Li, T.-T., Zhang, Y., Guo, J.-X., Lu, K.-K., Liu, W.-C., 2021b. CAND2/PMTR1 is required for melatonin-conferred osmotic stress tolerance in arabidopsis. Int. J. Math. Stat. 22, 4014. https://doi.org/10.3390/ijms22084014.

Wang, Q., Wu, Y., Ge, J., Xu, X., Lei, X., Wang, J., Wan, C., Wang, P., Gao, X., Gao, J., 2023a. Soil enzyme activities, physiological indicators, agronomic traits and yield of common buckwheat under herbicide combined with safeners. Sci. Total Environ. 903, 166261. https://doi.org/10.1016/j.scitotenv.2023.166261.

Wang, W., Zhang, F., Zhao, Q., Liu, C., Jim, C.Y., Johnson, V.C., Tan, M.L., 2023b. Determining the main contributing factors to nutrient concentration in rivers in arid northwest China using partial least squares structural equation modeling. J. Environ. Manag. 343, 118249. https://doi.org/10.1016/j.jenvman.2023.118249.

Wei, J., Li, D., Zhang, J., Shan, C., Rengel, Z., Song, Z., Chen, Q., 2018. Phytomelatonin receptor PMTR1-mediated signaling regulates stomatal closure in *Arabidopsis thaliana*. J. Pineal Res. 65, e12500. https://doi.org/10.1111/jpi.12500.

Weimer, A.K., Demidov, D., Lermontova, I., Beeckman, T., Van Damme, D., 2016. Aurora kinases throughout plant development. Trends Plant Sci. 21, 69–79. https://doi.org/10.1016/j.tplants.2015.10.001.

Yang, J., Ma, L., Di, S., Wang, Z., Quinet, M., Meng, Y., He, J., 2025. Exogenous rutin ameliorates NaCl-induced inhibition of fagopyrum esculentum germination and early growth. BMC Plant Biol. https://doi.org/10.1186/s12870-025-08002-7.

Yang, W.-J., Du, Y.-T., Zhou, Y.-B., Chen, J., Xu, Z.-S., Ma, Y.-Z., Chen, M., Min, D.-H., 2019. Overexpression of TaCOMT improves melatonin production and enhances drought tolerance in transgenic arabidopsis. Int. J. Math. Stat. 20, 652. https://doi.org/10.3390/ijms20030652.

Yuk, D., Jee, M.H., Koh, C.W., 2022. Simplified Y6-Based Nonfullerene Acceptors: In-Depth Study on Molecular Structure–Property Relation, Molecular Dynamics Simulation, and Charge Dynamics - Yuk - 2023 - Small. Wiley Online Library [WWW Document]. URL. https://onlinelibrary.wiley.com/doi/abs/10.1002/smll.202206547, 7.1.25.

Zhao, C., Yang, M., Wu, X., Wang, Y., Zhang, R., 2021. Physiological and transcriptomic analyses of the effects of exogenous melatonin on drought tolerance in maize (Zea mays L.). Plant Physiol. Biochem. 168, 128–142. https://doi.org/10.1016/j.plaphy.2021.09.044.

Zhu, J.-K., 2016. Abiotic stress signaling and responses in plants. Cell 167, 313–324. https://doi.org/10.1016/j.cell.2016.08.029.

Zuo, B., Zheng, X., He, P., Wang, L., Lei, Q., Feng, C., Zhou, J., Li, Q., Han, Z., Kong, J., 2014. Overexpression of *MzASMT* improves melatonin production and enhances drought tolerance in transgenic *Arabidopsis thaliana* plants. J. Pineal Res. 57, 408–417. https://doi.org/10.1111/jpi.12180.